JOURNAL OF CHEMICAL & ENGINEERING DATA

ARTICLE

pubs.acs.org/jced

Adsorption of Sulfate Ions from Aqueous Solution by Surfactant-Modified Palygorskite

Rui Dong,[†] Yuanfa Liu,[†] Xingguo Wang,[†] and Jianhua Huang*[,†,‡]

[†]State Key Laboratory of Food Science and Technology, School of Food Science and Technology, Jiangnan University, 1800 Lihu Road, Wuxi 214122, Jiangsu, P. R. China

[‡]Key Laboratory for Palygorskite Science and Applied Technology of Jiangsu Province, Huaiyin Institute of Technology, HuaiAn 223003, Jiangsu, P. R. China

ABSTRACT: The objectives of this work are to study palygorskite modified by a surfactant, octodecyltrimethylammonium chloride (OTMAC), and to study for the potential use of the surfactant-modified palygorskite (SMP) as an adsorbent for the adsorption of sulfate ions from aqueous solutions. The surface characters of SMP were undertaken by scanning electron microscopy (SEM), FTIR spectroscopy, X-ray photoelectron spectroscopy (XPS), and N_2 adsorption. The FTIR spectra and XPS showed that the surfactant (OTMAC) had effectively grafted on palygorskite. A batch technique was carried out to evaluate parameters affecting adsorption including pH, the amount of SMP, treatment time, and initial SO_4^{2-} concentration. The adsorption isotherms of SMP for sulfate ions were described by Langmuir, Freundlich, and Dubinin−Radushkevich equations, and the Freundlich model was best to express the adsorption process. The thermodynamic data indicated that the adsorption was an endothermic and spontaneous process. Results of kinetic experiments showed that the adsorption was best described by the pseudosecond-order kinetics model. Above all, the adsorption of sulfate ions extended the application of palygorskite to the removal of anions and wastewater purification.

1. INTRODUCTION

Sulfate ions are common anions in inorganic chemical industry, industrial wastewater, acid mine drainage, and drinking water. They mainly come from the processes of chemical weathering of sulfur-containing minerals and the oxidation of sulfides and sulfur. Sulfate ions are nontoxic and necessary for many kinds of organisms; however, they will cause an imbalance of the natural sulfur cycle and endanger human health when excessive ingested.[1] In addition, sulfate ions are corrosive to reinforced steel.[2] Several conventional methods for the removal of sulfate ions such as chemical precipitation, biological treatment, ion exchange, and adsorption technologies have been employed with different efficiencies.[3] Some of these methods have disadvantages and limitations. Precipitation, for example produces large amount of sludge in solution but biological treatment and ion exchange are costly. Alternatively, the adsorption method may be preferred for its rapid and high selectivity to remove sulfate ions, and sulfate can be recovered. The commonly used adsorbents include $BaCl_2$, $CaCl_2$, and $ZrO(OH)_2$, but $BaCl_2$ and $ZrO(OH)_2$ are expensive, and $BaCl_2$ will pollute the environment. Moreover, the removal efficiency by $CaCl_2$ is not high. Hence, it is necessary to develop a low-cost and effective anion adsorbent to remove sulfate ions.

In recent years, palygorskite has been paid attention as an alternative of conventional adsorbents on both the environmental and the economic points of view due to high surface area and a large number of silanol groups on its surface. Palygorskite is a hydrated magnesium silicate mineral with fibrous morphology, and possesses rectangular channels contained exchangeable Ca^{2+} and Mg^{2+} cations, zeolitic water, and water molecules bound to coordinative unsaturated metal ion centers, which situated at the edges of the ribbons.[4] However, natural palygorskite, which has permanent negative charges,[5] will produce repulsion toward anions, so surface modification by cationic surfactants is needed to reverse its surface charge if palygorskite is applied to anion adsorption. The modification of cationic surfactants on palygorskite and the potential application of such modified palygorskite as environmental remediation material have been studied previously.[5−8] However, there have been few reports on how surfactant-modified palygorskite (SMP) adsorb sulfate or other anion.

The main objectives of the present work were to study sulfate ions adsorption by SMP, which was freshly prepared in relatively simple and well-controlled laboratory system; to investigate the effects of the parameters, such as temperature, pH, amount of SMP, treatment time, and initial concentration of sulfate ions; to evaluate the kinetic and thermodynamic (entropy, enthalpy, free energy) parameters of sulfate adsorption on SMP; and to discuss the mechanism of sulfate ions interaction with SMP, which were essential in studying their adsorption behavior at the interface.

2. MATERIALS AND METHODS

2.1. Materials. The surfactant octodecyltrimethylammonium chloride (OTMAC) with a purity of 70.0 % was obtained from the Feixiang Chemical Co. (China). The palygorskite from Oilbetter Co. (China) with a particle size of 200-mesh screened as reported was used to SMP preparation.[9] Reagents in all cases were of analytical grade or better and were used without additional purification. A stock solution of sulfate was prepared by dissolving 1.8125 g of K_2SO_4 in 1 kg deionized water (DIW)

Received: June 20, 2011
Accepted: August 2, 2011
Published: September 07, 2011

($c(SO_4^{2-})$ =1 g·kg^{-1}). Secondary stock solutions of 100 mg·kg^{-1} SO_4^{2-} were prepared weekly and used to test the solution.

2.2. Preparation of SMP. *2.2.1. HCl Treatment.* A sample of 10 g of palygorskite was ground to colloidal size and transferred to a 250 mL round bottomed flask. Then 2 mol·kg^{-1} hydrochloric acid was added until the total volume was 100 mL. The mixtures were refluxed for 2 h at 343 K. Then, excess HCl was removed by washing with DIW until $AgNO_3$ test for chloride was negative and pH 7.0 was achieved.

2.2.2. OTMAC Modified Palygorskite. The mixture of palygorskite and OTMAC solution was sonicated. Ultrasonic wave can greatly improve the rate of SMP preparation. The sonication conditions were as follows: the ratio of adding OTMAC and palygorskite was 14.9 g/100 g, the treatment time was 11 min, and the plate current was 0.6 A. Then, the separated SMP was washed repeatedly to remove the water-soluble particle. The product was dried at 378 K to constant mass in evaporating dishes and sieved to similar particle sizes. This produced a uniform material for the complete set of adsorption tests which was stored in an airtight plastic container for the following experiments. The CHN analysis showed that nitrogen content of the product attained 0.18 %, indicating that OTMAC content was 4.46 %. According to eq 1, the grafting ratio was 44.7 %.

$$\text{grafting ratio} = \frac{W_1}{W_2} \cdot 100\ \% \tag{1}$$

where W_1 is the mass of OTMAC grafted to palygorskite and W_2 is the initial dosage of OTMAC added to natural palygorskite.

2.3. Experiments and Methods of Characterization. Scanning electron microscopy (SEM), Fourier transform infrared spectroscopy (FTIR), X-ray photoelectron spectroscopy (XPS), N_2 adsorption, and CS analysis were undertaken to understand of SMP's structures and confirm that OTMAC adsorbed onto palygorskite and SO_4^{2-} adsorbed onto SMP and discuss the mechanism of adsorption of SO_4^{2-} onto SMP.

The amount of OTMAC adsorbed onto palygorskite was determined by CHN analysis (Vario EL III, Elementar). A FEI Sirion 200 scanning electron microscope (SEM) was employed to characterize SMP for its morphological information. The FTIR spectra were recorded on a 470-IR spectrometer (Japan), samples being examined in the form of KBr disks. XPS was conducted on an ESCALAB 250 spectrometer (Thermo-VG Scientific) using monochromatic Al Kα radiation ($2.38 \cdot 10^{-16}$ J). The surface areas and porosity analysis were obtained from nitrogen adsorption/desorption in a micromeritics surface analyzer system (Micromeritics Tristar II 3020), employing Brunauer–Emmett–Teller (BET) methods. Sulfur content of SMP after adsorption was determined by combustion and infrared detection of inorganic material (LECO, CS-600, USA).

2.4. Adsorption Procedure. All of the adsorption experiments were carried out in 250 mL iodine flasks by adding a given amount of palygorskite or modified palygorskite to 50 g different concentrations of sulfate solution and shaking in a shaking thermostatic bath at 150 rpm for a given time. Preliminary experiments were conducted for various time intervals to determine when adsorption equilibrium was reached. The result showed that 360 min was enough for adsorption equilibrium. Thus, kinetics and the effects of treatment time on adsorption were determined in the range of (0 to 360) min and an initial sulfate concentration of 50 mg·kg^{-1} with a ratio of solid to liquid of 10 g·kg^{-1}. Adsorption isotherms were studied in the range of (20 to 130) mg·kg^{-1} at different temperatures [(308, 328, and 348) K]. The pH value of suspension was adjusted with dilute HCl or NaOH solution (pH values determined by Mettler Toledo 320 pH meter). The solid and liquid phases were separated by centrifugation at 4000 rpm for 10 min after adsorption. The concentration of sulfate was determined at the wavelength of 420 nm using a UV–visible spectrophotometer.[10] The coefficient of determination (R^2) for standard curves was no less than 0.999. The adsorption capacity and removal percentage (%) were calculated according to the following eqs 2 and 3:

$$q = \frac{(C_0 - C_e) \cdot M}{W} \tag{2}$$

$$\text{removal percentage } (r)\% = \frac{C_0 - C_e}{C_0} \cdot 100\ \% \tag{3}$$

where q is the SO_4^{2-} adsorption capacity per gram; C_0 is the initial concentration of SO_4^{2-} (mg·kg^{-1}); C_e is the equilibrium SO_4^{2-} concentration in solution (mg·kg^{-1}); W is the mass of adsorbent used (g), and M is the mass of SO_4^{2-} solution (kg). All experiments were run repeatedly, and only mean values were presented to ensure reproducibility. All glassware and the polyethylene vials were acid-washed for at least 12 h before each experiment, then washed with DIW several times, and dried.

3. RESULTS AND DISCUSSION

3.1. Adsorbent Characterization. *3.1.1. Scanning Electron Microscopy (SEM).* SEM is a primary tool for characterizing the surface morphology and fundamental physical properties of the adsorbent. SEM images of natural palygorskite, SMP, are shown in Figure 1. Natural palygorskite showed bundles of close packed fibers, and the diameter of each fiber was about 50 nm. After the modification, the diameter of each SMP became larger, and some aggregated together due to OTMAC covering on the surface of palygorskite.

3.1.2. Results of FTIR. The FTIR characterization of natural palygorskite, acid-activated palygorskite, and SMP are shown in Figure 2. The band around 3614 cm^{-1} was assigned to stretching vibration of Al–OH and (Al–Fe)–OH, which was the character of palygorskite, and its intensity was related to higher Al octahedral content and lower Mg content. The band around 3556 cm^{-1} was attributed to bonded water coordinated to Fe and Al. The broad bands at 3407 cm^{-1} was ascribed to zeolitic water, and the Si–O–Si stretching band appeared at 1025 cm^{-1}. The band at 1641 cm^{-1} for natural palygorskite was assigned to zeolitic water.[11] The band at 1427 cm^{-1} and a shoulder at 876 cm^{-1} were assigned to calcite, which disappeared after acid treatment. The medium intensity and sharp band at 778 cm^{-1} were designated to quartz, which also existed after modification.[12] The additional peaks at (2852 and 2924) cm^{-1}, which were absent in palygorskite, suggested the presence of C–H stretching bands of both CH_3 and CH_2 groups of OTMAC. A weak band at around 1467 cm^{-1} of SMP was attributed to C–N stretching vibration, indicating the presence of alkyl ammonium.[13,14]

3.1.3. XPS Analysis. The full XPS spectra (Figure 3) were used to verify elements present on the surface of particles and their bonding states, such Al 2p, Si 2p, N 1s, C 1s, O 1s, and others. It can be clearly seen that the carbon content increased from 8.1 % to 20.3 %. In addition, a new peak at about $6.43 \cdot 10^{-17}$ J in SMP was attributed to N 1s, which confirmed that OTMAC had

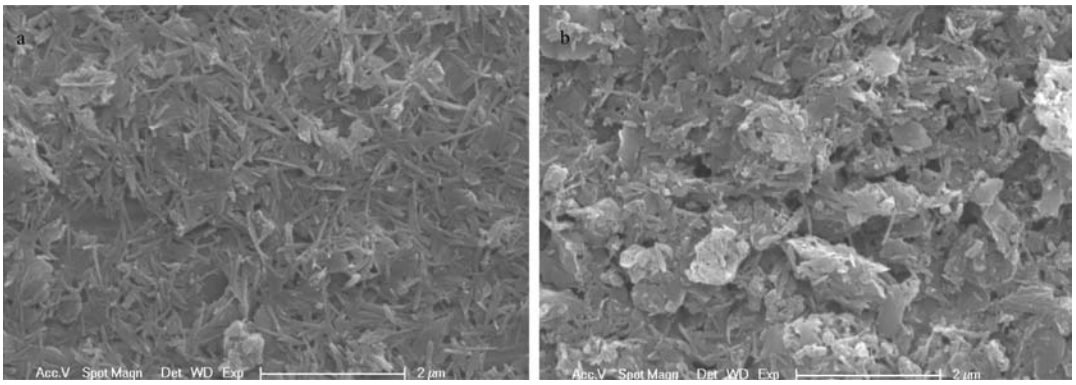

Figure 1. SEM images of (a) natural palygorskite and (b) SMP.

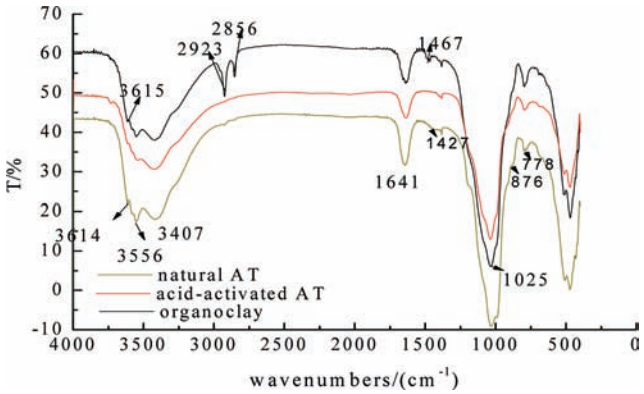

Figure 2. FTIR spectra of natural and acid-activated palygorskite and SMP.

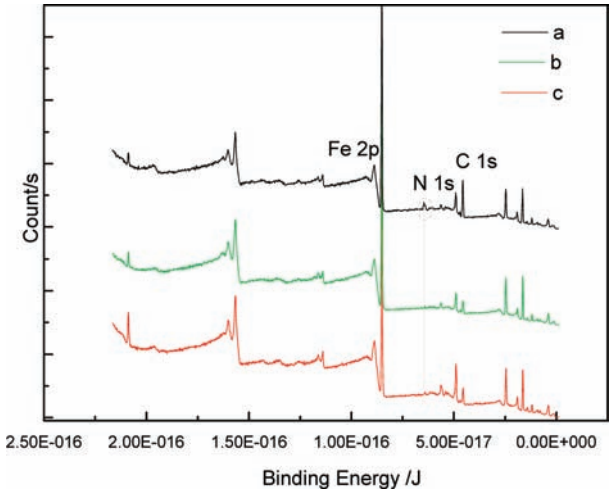

Figure 3. XPS survey spectra of (a) natural palygorskite, (b) acid-activated palygorskite, and (c) SMP.

successfully grafted on palygorskite.[13] The same result was also obtained in CHN data and FTIR (Figure 2).

3.1.4. N_2 Adsorption. The specific surface areas, pore sizes, and micropore areas of the natural palygorskite, acid-activated palygorskite, and SMP are listed in Table 1. The surface areas were determined from the adsorbed nitrogen volume. The value of surface area (calculated by application of BET equation) greatly increased after HCl treatment. As the acid attack processed, more

Table 1. Textural Characteristics of Natural Palygorskite, Acid-Activated Palygorskite, and SMP

materials	surface area $m^2 \cdot g^{-1}$	average pore diameter $4\ V \cdot A^{-1}$	micropore area by t-plot $m^2 \cdot g^{-1}$
natural palygorskite	155	93	20
acid-activated	254	88	67
SMP	130	96	–

mesoporosity and microporosity were created; the possible reasons were that fibrous bundles disaggregated initially, and then the octahedral cations (Mg(II) and Al(III)) dissolved.[15−17] According to the *t*-plot, the micropore area of acid activated palygorskite was about 70 $m^2 \cdot g^{-1}$, which was bigger than 20 $m^2 \cdot g^{-1}$ of natural palygorskite. Because SMP was covered by long-chain alkyl reduced the adsorption of N_2, the surface area of SMP was smaller. SMP had the largest pore diameter, probably because the distance between each OTMAC molecule covered on the surface was longer, while acid-activated palygorskite had a relatively smaller pore diameter due to acid attack.

3.2. Adsorption Experiment. To investigate the best adsorption efficiency of SO_4^{2-} on SMP, several parameters were studied such as pH, SMP dosage, and treatment time.

3.2.1. Comparison of Natural Palygorskite and Modified Palygorskite. To assess the adsorption capacity and adsorption rate, three adsorbents, namely, natural palygorskite, acid-activated palygorskite, and SMP were used for comparison purposes. The removal percentage of SO_4^{2-} was achieved by about 500 mg of natural palygorskite, acid-activated palygorskite, and SMP, from 50 g of solution containing 50 $mg \cdot kg^{-1}$ SO_4^{2-}, respectively. The result showed that SMP was 10 times more effective than natural palygorskite and acid-activated palygorskite. The reason was that there was repulsion between SO_4^{2-} and natural palygorskite and acid-activated palygorskite, since they possessed permanent negative charges. In addition, acid-activated palygorskite was a little more effective than natural palygorskite, which may result from less negative charges of adsorbent surface after treatment with HCl.[18]

For SMP, there was electrostatic force between the positively charged surface of the adsorbate and the negatively charged sulfate ions. OTMAC molecular strongly grafted on palygorskite first; second, other OTMAC molecules interacted with the first layer OTMAC through hydrophobic force, formed a double-layer

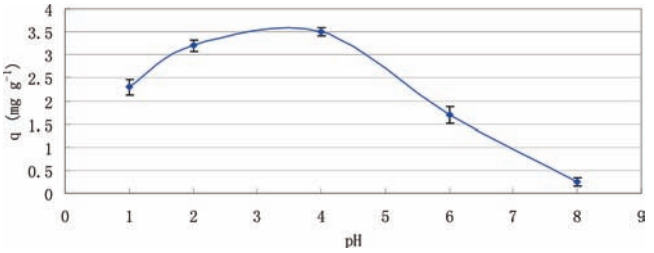

Figure 4. Effect of pH on content removal of SO_4^{2-} by SMP.

structure, and thus reversed the surface charge.[19] SO_4^{2-} adsorption was mainly due to ion exchange with Cl^- attached to alkyl ammonium with electrostatic forces as the following equation:

$$2\text{OTMAC-palygorskite}\cdots\text{Cl} + SO_4^{2-} = (\text{OTMAC-palygorskite})_2\cdots SO_4 + 2Cl^- \quad (4)$$

where the dots represent that there was physical force between them instead of chemical force. There might be other forces between SO_4^{2-} and SMP except electrostatic forces. Complexes could form between sulfate ions and Fe and Al on the SMP surface, which were brought by acid treatment. These complexes could be described simply as ═Fe—O—SO_2—O—Fe═ and ═AlO—SO_2—O—Al═.[20,21] However, adsorption caused by this mechanism consisted of a rather small amount of content in the total adsorption.

3.2.2. Effect of pH. The variation of pH was an important parameter in the adsorption process because it would affect the electrical properties of SMP. The effect of the pH of initial suspension on the sulfate adsorption is presented in Figure 4. The adsorption capacity increased at a slow rate in pH ranging from 1 to 4 and then decreased drastically as the solution became neutral and basic.

The reason for the optimum pH was that the surface of adsorbent was highly protonated in acidic medium and tended to adsorb negative ions. Furthermore, more OH^- competed with SO_4^{2-} at higher pH; thereby, low removal content was obtained above pH 6. Other anion adsorption experiments had similar conclusions.[22,23] While too many H^+ ions would influence the stability of SMP, the suitable pH of initial suspension was about 4. Therefore, all further studies were carried out at pH 4.

3.2.3. Effect of the SMP Dosage. To investigate the effect of adsorbent amount on the removal of sulfate ions, a series of experiments were performed for various SMP doses. Batch experiments were conducted using 50 g of sulfate solution, adding different amounts of SMP [(200 to 710) mg] at a fixed pH (pH = 4), temperature (308 K), and sulfate concentration (50 mg·kg^{-1}). Figure 5 showed that the removal percentage increased with the increase in the dose of adsorbent, yet the sulfate ions adsorbed per gram decreased. Thus the addition of SMP was 0.4 g in further experiments.

3.2.4. Effect of Treatment Time. The treatment time was found by taking subsamples from the flasks for 6 h at intervals and analyzing the supernatants for sulfate ions with a fixed adsorbent dose (0.4 g), fixed pH (4.0), and 308 K. The removal of sulfate ions increased rapidly with time increasing and then continued at a relatively slow rate and reached saturation in about 240 min. Therefore, considering economic and practical aspects, the treatment time of 240 min was employed in its further application.

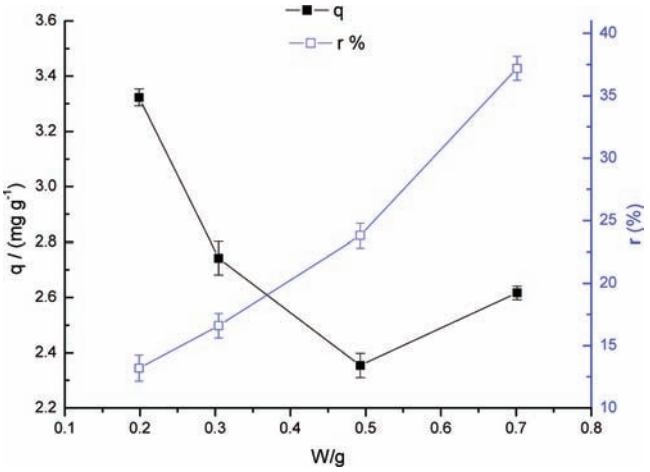

Figure 5. Effect of SMP addition on adsorption.

On the basis of the above tests, the optimal experimental adsorption conditions were the following: SMP addition, 0.4 g; pH of initial suspension, 4.0; and treatment time, 240 min. The SO_4^{2-} content of SMP which had adsorbed sulfate ions in the above condition determined by CS analyzer was 3.25 mg·g^{-1}, which is coincident with q calculated by the above-mentioned equation.

3.3. Equilibrium Experiments. Batch experiments were conducted under the optimum conditions, with the initial SO_4^{2-} concentration varying as (20, 30, 40, 50, 70, 90, 100, 120, and 130) mg·kg^{-1}. The SO_4^{2-} adsorption experiments were done in duplicate for each anion concentration. The difference between two measurements did not exceed 10 %.

To optimize the design of the system to adsorb SO_4^{2-}, it was important to select an appropriate adsorption isotherm to fit to the equilibrium data. The most commonly used isotherm is the Langmuir model,[24] in which model adsorption is limited by surface site saturation,

$$q = \frac{bq_m C_e}{1 + bC_e} \quad (5)$$

where q_m is the monolayer adsorption capacity of the adsorbent (mg·g^{-1}), and b is the bonding energy coefficient (kg·mg^{-1}) related to the free energy of adsorption. Values of the essential characteristics of Langmuir isotherm could be expressed by a dimensionless constant called the equilibrium parameter (R_L):[25]

$$R_L = \frac{1}{1 + bC_0} \quad (6)$$

where C_0 (mg·kg^{-1}) is the highest initial concentration of adsorbent and b (kg·mg^{-1}) is the Langmuir constant.

Meanwhile, the Freundlich model assumes a heterogeneous adsorption surface with sites that have different energies of adsorption and are not equally available.[26] The Freundlich isotherm is given by:

$$q_e = K_F C_e^{1/n} \quad (7)$$

where K_F and $1/n$ (dimensionless) are the Freundlich constants. K_F is related to the adsorption capacity, and $1/n$ is related to the adsorption intensity, which varies with the heterogeneity of the adsorption material.

Table 2. Langmuir, Freundlich, and D-R Isotherm Parameters

	Langmuir			Freundlich			D-R			
T	q_m	b					Q_m	β	E	
K	mg·g^{-1}	kg·mg^{-1}	R^2	K_F	$1/n$	R^2	mg·g^{-1}	kJ^2·mol^{-2}	kJ·mol^{-1}	R^2
308	3.24	0.18	0.95	1.20	0.21	0.99	2.95	2.23	0.48	0.77
328	2.56	0.26	0.90	1.26	0.16	0.97	2.38	1.70	0.55	0.74
348	2.11	0.39	0.75	1.22	0.12	0.95	2.08	0.98	0.71	0.55

The Dubinin−Radushkevich (D-R) isotherm can be used to describe adsorption on both homogeneous and heterogeneous surfaces,[27] which can be described as:

$$q = Q_m \exp(-\beta\varepsilon^2) \quad (8)$$

$$\varepsilon = RT \ln(1 + 1/C_e) \quad (9)$$

where Q_m is the theoretical saturation adsorption capacity in the D-R equation; β is the activity coefficient related to mean adsorption energy (mol^2·kJ^{-2}); ε is the Polanyi potential; R equals to ideal gas constant (8.314 J·mol^{-1}·K^{-1}); T is the absolute temperature (K). The D-R isotherm is based on the Polanyi−Manes adsorption theory, which can predict solute adsorption onto organoclay.[28]

The isotherm constants and correlation coefficients calculated from the nonlinear Langmuir, Freundlich, and D-R plots are presented in Table 2. Unlike the linear analysis, a different isotherm form would affect R^2 and the final determination of parameters significantly, and nonlinear methods would prevent such errors.[29] It was found that the adsorption conformed to Freundlich more than other isotherms. This suggested that the adsorption took place at heterogeneous sites, while it also conformed to Langmuir isotherm at (308 and 328) K (R^2 > 0.89),[30] which implied that both monolayer adsorption and heterogeneous surfaces conditions existed at low temperature.

The value of q_m in Langmuir isotherm model showed that the highest adsorption capacity was 3.24 mg·g^{-1}. The observed adsorption capacity decreased with increasing temperature, which may be due to a tendency for SO_4^{2-} ions to escape from the solid phase to the bulk phase with an increase in the temperature of the solutions. This suggested the weakening of adsorptive forces between the active sites of the adsorbent and adsorbate and between the adjacent molecules of the adsorbed phase with the rise of temperature.

The adsorption is unfavorable if R_L is above 1, while the value of R_L < 1 represents favorable adsorption. In this study, the value of R_L was between 0 and 1 at the temperatures studied showing that the adsorption of sulfate ions was favorable. The Freundlich constants $1/n$ was far below unity suggested the adsorption was a favorable physical process.[31]

The mean free energy of adsorption (E), defined as the free energy change when 1 mol of ions are transferred to the surface of the solid from infinity in solution, can be calculated from the activity coefficient (β) using the following equation:

$$E = (-2\beta)^{-0.5} \quad (10)$$

Although the adsorption process did not conform to the D-R isotherm, the E value was calculated as 0.48 kJ mol^{-1} at 308 K which was far below 8 kJ·mol^{-1}, indicating that the adsorption process was a physical interaction process (van der Waals interaction) and mainly controlled by the electrostatic force between positive site of the adsorbent and the negative charged SO_4^{2-} rather than a strong chemical bond.[32]

Table 3. Thermodynamic Parameters of SO_4^{2-} Adsorption, with Uncertainties at a 0.95 Confidence Level

T		ΔG^0	ΔH^0	ΔS^0
K	K_d	kJ·mol^{-1}	kJ·mol^{-1}	J·mol^{-1}·K^{-1}
308	1.42 ± 0.10	−0.90 ± 0.16		
328	2.73 ± 0.30	−2.74 ± 0.30	23.8 ± 0.5	80.5 ± 1.4
348	4.12 ± 0.20	−4.10 ± 0.14		

3.4. Adsorption Thermodynamics. The value of thermodynamic equilibrium constants (K_d) of the adsorption process was the intercept of plotting $\ln(q/C_e)$ versus q.[27] When the reaction reaches equilibrium, Gibbs free energy (ΔG) becomes zero so that ΔG^0 equals to $-RT \ln K_d$.

$$\Delta G^0 = -RT \ln K_d \quad (11)$$

The standard enthalpic changes (ΔH^0) and entropy change (ΔS^0) can be calculated as follows:

$$\ln K_d = \frac{\Delta S^0}{R} - \frac{\Delta H^0}{RT} \quad (12)$$

The parameters of the adsorption are shown in Table 3. The value of ΔH^0 was positive showed that the process was endothermic and the product was energetically stable. The value of free energy (ΔG^0) was between −20 and 0 kJ mol^{-1} indicated the adsorption was a spontaneous physical process.[33] The similar spontaneous endothermic reactions were also observed in dye 161 adsorption using bamboo activated carbons,[34] adsorption of methylene blue adsorption onto NaOH-modified rejected tea and etc. ΔG^0 decreased at higher temperature, which suggested that the spontaneity of the process increased with raising in temperature.[35,36] The positive values of ΔS^0 reflected the affinity of SMP toward SO_4^{2-} in aqueous solution and the increased randomness at solid/solution interface during the adsorption process. The positive entropy was probably due to the structural change of SMP. It would turn more random once SO_4^{2-} adsorbed onto it. This might be related to negatively changed ions rather than sulfate specificity. The positive ΔS^0 might suggest that ion-exchange and replacement reactions also occurred in the creation of steric hindrance.[37]

3.5. Adsorption Kinetics. To determine the dynamic characteristics of SO_4^{2-}, the first-order kinetics equation was tested, but straight lines were not obtained. Then, we tried pseudosecond-order model by plotting t/q_t versus t and the intraparticle diffusion equation.[38,39] Their linear forms are as

Table 4. Kinetic Parameters of the Adsorption Process

	pseudosecond-order kinetic model				intraparticle diffusion model			pseudofirst-order kinetics	
T	q_e	k	h		k_p			K_{pfo}	
K	mg·g^{-1}	mg·g^{-1}·min^{-1}	mg·g^{-1}·min^{-1}	R^2_{pso}	mg·g^{-1}·min$^{-0.5}$	C	R_p^2	min^{-1}	R^2_{pfo}
308	3.35	0.08	0.94	0.99	0.07	2.27	0.83	−0.011	0.89
328	2.48	1.01	6.21	0.99	0.03	2.05	0.55	−0.006	0.09
348	2.12	2.42	10.83	0.99	0.02	1.83	0.39	−0.007	0.33

follows:

$$\text{pseudofirst-order}: \log\frac{q_e}{(q_e - q_t)} = -\frac{K_{pfo}t}{2.303} \quad (13)$$

$$\text{pseudosecond-order}: \frac{t}{q_t} = \frac{1}{kq_e^2} + \frac{1}{q_e}t \quad (14)$$

$$\text{intraparticle diffusion}: q_t = k_p t^{0.5} + C \quad (15)$$

The initial adsorption rate can be obtained as q_t/t approaches zero:

$$h = q_e^2 \cdot k \quad (16)$$

where k (mg·g^{-1}·min^{-1}) is the adsorption rate constant of pseudosecond order; h is the initial adsorption rate (mg·g^{-1}·min^{-1}); q_t is the amount of SO_4^{2-} adsorbed at time t; q_e is the amount of SO_4^{2-} adsorbed at equilibrium; K_{pfo} is the constant in pseudofirst-order; k_p is the intraparticle diffusion rate constant; C is the constant in the intraparticle diffusion model, which is proportional to the boundary layer thickness. In intraparticle diffusion equation, if the plot of q_t versus $t^{0.5}$ is linear and it passes through the origin, then the intraparticle diffusion would be the sole rate-limiting process.

The rate parameters k and q_e can be directly obtained from the intercept and slope of the plot of t/q_t against t. The values of k and h of different temperatures are listed in Table 4. A good correlation coefficient (R^2_{pso}) was obtained for the pseudosecond-order kinetic model, which indicated that SO_4^{2-} adsorption onto SMP followed the pseudosecond-order rate expression. The values of the pseudosecond-order rate constant k were found to increase from (0.08 to 2.42) mg·g^{-1}·min^{-1} with an increase in temperature from (308 to 348) K, which meant that the adsorption rate increased with the increase of temperature. Meanwhile, the amount of SO_4^{2-} adsorbed at equilibrium decreased from (3.35 to 2.12) mg·g^{-1} with the temperature increase.

The correlation coefficient (R_d^2) of intraparticle diffusion model in this study indicated the adsorption of sulfate ions onto SMP did not follow the intraparticle diffusion kinetics. However, the plot of q_t versus $t^{0.5}$ can be divided into a multilinearity correlation. Take the plot at 308 K, for example; Figure 6 showed that three stages occurred during the adsorption process. For the first sharp stage, that is, from (0 to 1) min, sulfate ions were transported to the external surface through film diffusion, and k_p = 2.1 mg·g^{-1}·min$^{-0.5}$ illustrated the process was very fast. The second stage was the gradual adsorption stage where intraparticle diffusion was rate-limiting, k_p = 0.15 mg·g^{-1}·min$^{-0.5}$. The third stage was the final equilibrium stage where the intraparticle diffusion started to slow down due to the extremely low solute concentration in solution.

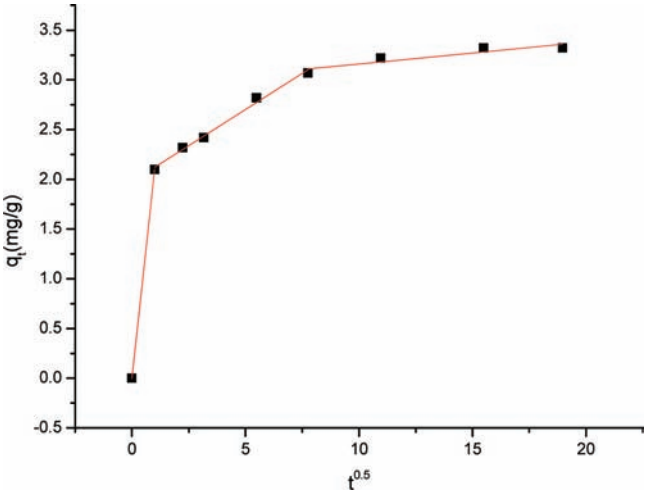

Figure 6. Intraparticle diffusion plots for the adsorption of sulfate ions onto SMP at 308 K.

4. CONCLUSIONS

This study was focused on palygorskite, which was used to adsorb sulfate ions after modification by the surfactant OTMAC. The characteristic analysis indicated that OTMAC had successfully grafted on palygorskite. Compared with natural palygorskite and acid-activated palygorskite, SMP was more effective than others. It is, therefore, possible to be used in the treatment of SO_4^{2-} solution. The operating parameters such as SMP addition, pH of initial suspension, and contact time were effective on the adsorption efficiency of sulfate ions. The equilibrium studies showed that the adsorption took place on both homogeneous and heterogeneous sites, and the maximum adsorption capacity was 3.24 mg·g^{-1}. The adsorption kinetics demonstrated that the adsorption process of SO_4^{2-} onto SMP closely followed a pseudosecond-order kinetic model, and the intraparticle diffusion model showed that film diffusion and intraparticle diffusion simultaneously operated in the adsorption process. On the basis of the research, the force between sulfate ions and SMP was van der Waals interaction. It is concluded that SMP is an effective and alternative adsorbent for the removal of sulfate ions in terms of natural and abundant availability and low cost.

AUTHOR INFORMATION

Corresponding Author

*Telephone: (086)510-85876799; fax: (086)510-85876799; e-mail: huangjianhua1124@sina.com.cn.

Funding Sources

The authors express their gratitude to the support provided by the National Natural Science Foundation of China (Contract No: 50902060), the Project of Science and Technology of JiangSu Province (Contract No: BE2009014), and the Foundation of Key Laboratory of Attpulgite Science and Applied Technology of Jiangsu Province (Contract No: HPK200902).

REFERENCES

(1) Silva, A. J.; Varesche, M. B.; Foresti, E.; Zaiat, M. Sulfate removal from industrial wastewater using a packed-bed anaerobic reactor. *Process Biochem.* **2002**, *37*, 927–935.

(2) Al-Tayyib, A. J.; Khan, M. S. Effect of sulfate ions on the corrosion of rebars embedded in concrete. *Cem. Concr. Compos.* **1991**, *13*, 123–127.

(3) Cao, W.; Zhi, D.; Zhou, X.; Yi, X.; Wu, P.; Zhu, N.; Lu, G. Removal of sulfate from aqueous solution using modified rice straw: Preparation, Characterization and adsorption performance. *Carbohydr. Polym.* **2011**, *85*, 571–577.

(4) Bradley, W. F. Structure scheme of attapulgite. *Am. Mineral.* **1940**, *25*, 405.

(5) Ozcan, A.; Sahin, M.; Ozcan, A. S. Adsorption of nitrate ions onto sepiolite and surfactant-modified sepiolite. *Adsorpt. Sci. Technol.* **2005**, *23*, 323–334.

(6) Huang, J.; Liu, Y.; Jin, A.; Wang, X.; Yang, J. Adsorption studies of a water soluble dye, reactive red MF-3B, using sonication-surfactant-modified palygorskite clay. *J. Hazard. Mater.* **2007**, *143*, 541–548.

(7) Li, Z. H.; Willams, C. A.; Kniola, K. Removal of anionic contaminant using surfactant-modified palygorskite and sepiolite. *Clays Clay Miner.* **2005**, *51*, 445–451.

(8) Sarkar, B.; Xi, Y.; Megharaj, M.; Naidu, R. Orange II adsorption on palygorskites modified with alkyl trimethylammonium and dialkyl dimethylammonium bromide- An isothermal and kinetic study. *Appl. Clay Sci.* **2011**, *51*, 370–374.

(9) Huang, J.; Wang, X.; Jin, Q. Removal of phenol from aqueous solution by adsorption onto OTMAC-modified attapulgite. *J. Environ. Eng.* **2007**, *84*, 229–236.

(10) *Water and wastewater monitoring analysis method*, 4th ed.; State Environmental Protection Adminsstration of China: China, Beijing, 2002.

(11) Suarez, M.; Romero, E. G. FTIR spectroscopic study of palygorskite: Influence of the composition of the octahedral sheet. *Appl. Clay Sci.* **2006**, *31*, 154–163.

(12) Cai, Y.; Xue, J.; Polya, D. A. A Fourier transform infrared spectroscopic study of Mg-rich, Mg-poor and acid leached palygorskites. *Spectrochim. Acta, Part A* **2007**, *66*, 282–288.

(13) Zhang, L.; Jin, Q.; Huang, J.; Liu, Y.; Wang, X. Modification of palygorskite surface by organofunctionalization for application in immobilization of $H_3PW_{12}O_{40}$. *Appl. Clay Sci.* **2010**, *256*, 5911–5917.

(14) Anirudhan, T. S.; Ramachandran, M. Adsorptive removal of tannin from aqueous solutions by cationic surfactant-modified bentonite clay. *J. Colliod Interface Sci.* **2006**, *299*, 116–124.

(15) Gonzalez, F.; Pesquera, C.; Benito, I. Mechanism of acid activation of magnesic palygorskite. *Clays Clay Miner.* **1989**, *37*, 258–268.

(16) Liu, Y.; Dai, W.; Ting, W.; Yong, T. Superficial performance and pore structure of palygorskite treated by hydrochloric acid. *J. Cent. South. Univ. Technol.* **2006**, *13*, 451–455.

(17) Gonzalez, F.; Pesquera, C.; Blanco, C.; Benito, I.; Mendioroz, S.; Pajares, J. A. Structural and textural evolution under thermal treatment of natural and acid-acivated Al-rich and Mg-rich palygorskite. *Appl. Clay Sci.* **1990**, *5*, 23–36.

(18) Ye, H.; Chen, F.; Sheng, Y.; Sheng, G.; Fu, J. Adsorption of phosphate from aqueous solution onto modified palygorskites. *Sep. Sci. Technol.* **2006**, *50*, 283–290.

(19) Alkaram, U. F.; Mukhis, A. A.; Al-Dujaili, A. H. The removal of phenol from aqueous solutions by adsorption using surfactant-modified bentonite and kaolinite. *J. Hazard. Mater.* **2009**, *169*, 324–332.

(20) Parifitt, R. L.; Smart, R. St. C. Infrared spectra from binuclear bridging complexes of sulfate adsorbed on goethite (α-FeOOH). *J. Chem. Soc.* **1977**, *73*, 796–802.

(21) Rao, S. M.; Sridharan, A. Mechanism of sulfate adsorption by kaolinite. *Clays Clay Miner.* **1984**, *32*, 414–418.

(22) Nodvin, S. C.; Driscoll, C. T.; Likens, G. E. The effect of pH on sulfate adsorption by a forest soil. *Soil Sci.* **1986**, *142*, 69–75.

(23) Mahramanlioglu, M.; Kizilcikli, I.; Bicer, I. O. Adsorption of fluoride from aqueous solution by acid treated spent bleaching earth. *J. Fluorine Chem.* **2002**, *115*, 41–47.

(24) Langmuir, I. The constitution and fundamental properties of solids and liquids. *J. Am. Chem. Soc.* **1916**, *38*, 2221–2295.

(25) Hameed, B. H.; Krishni, R. R.; Sata, S. A. A novel agricultural waste adsorbent for the removal of cationic dye from aqueous solutions. *J. Hazard. Mater.* **2009**, *162*, 305–311.

(26) Zheng, Y.; Zhang, J.; Wang., A. Fast removal of ammonium nitrogen from aqueous solution using chitosan-g-poly (acrylic acid)/attapulgite composite. *Chem. Eng. J.* **2009**, *155*, 215–222.

(27) Lyubchik, S. I.; Lyubchik, A. I.; Galushko, O. L.; Tikhonova, L. P.; Vital, J.; Fonseca, I. M.; Lyubchik, S. B. Kinetics and thermodynamics of the Cr (III) adsorption on the activated carbon from commingled wastes. *Colloid Surf., A.* **2004**, *242*, 151–158.

(28) Fuller, M.; Smith, J. A.; Burns, S. E. Sorption of nonionic organic solutes from water to tetraalkylammonium bentonites: Mechanistic considerations and application of the Polanyi-Manes potential theory. *J. Colloid Interface Sci.* **2007**, *313*, 405–413.

(29) Parimal, S.; Prasad, M.; Bhaskar, U. Prediction of equilibrium sorption isotherm: comparison of linear and nonlinear methods. *Ind. Eng. Chem. Res.* **2010**, *49*, 2882–2888.

(30) Jaynes, W. F.; Boyd, S. A. Hydrophobicity of siloxane surfaces in smectites as revealed by aromatic hydrocarbon adsorption from water. *Clay Clay Miner.* **1991**, *39*, 428–436.

(31) Jiang, J. Q.; Cooper, C.; Ouki, S. Comparison of modified montmorillonite adsorbents. Part I. Preparation, characterization and phenol adsorption. *Chemosphere* **2002**, *47*, 711–716.

(32) Hu, B; Luo, H.; Chen, H.; Dong, T. Adsorption of chromate and para-nitrochlorobenzene on inorganic-organic montmorillonite. *Appl. Clay Sci.* **2011**, *51*, 198–201.

(33) Weng, C. H.; Tsai, C. Z.; Chu, S. H.; Sharma, Y. C. Adsorption characteristics of copper (II) onto spent activated clay. *Sep. Purif. Technol.* **2007**, *54*, 187–197.

(34) Wang, L.; Yan, G. Adsorptive removal of direct yellow 161 dye from aqueous solution using bamboo charcoals activated with different chemicals. *Desalination* **2011**, *274*, 81–90.

(35) Nasuha, N.; Hameed, B. H. Adsorption of methylene blue from aqueous solution onto NaOH-modified rejected tea. *Chem. Eng. J.* **2011**, *166*, 783–786.

(36) Chen, H.; Zhao, Y.; Wang, A. Removal of Cu(II) from aqueous solution by adsorption onto acid-activated palygorskite. *J. Hazard. Mater.* **2007**, *149*, 346–354.

(37) Unuabonah, E. I.; Adebowale, K. O.; Olu-Owolabi, B. I. Kinetic and thermodynamic studies of the adsorption of lead (II) ions onto phosphate-modified kaolinite clay. *J. Hazard. Mater.* **2007**, *144*, 386–395.

(38) Ho, Y. S.; Key, G. M. Pseudo-second order model for sorption processes. *Process Biochem.* **1999**, *34*, 451–465.

(39) Raji, C.; Anirudhan, T. S. Batch Cr (VI) removal by polyacrylamide-grafted sawdust: kinetics and thermodynamics. *Water Res.* **1998**, *32*, 3772–3780.